A mathematical model predicting the coculture dynamics of endothelial and mesenchymal stem cells for tissue regeneration

Wang, Yao; Bronshtein, Tomer; Sarig, Udi; Nguyen, Evelyne Bao-Vi; Boey, Freddy Yin Chiang; Venkatraman, Subbu S.; Machluf, Marcelle

2013

Wang, Y., Bronshtein, T., Sarig, U., Nguyen, E. B.-V., Boey, F. Y. C., Venkatraman, S. S., et al. (2013). A mathematical model predicting the coculture dynamics of endothelial and mesenchymal stem cells for tissue regeneration. Tissue engineering part A, 19(9-10), 1155-1164.

https://hdl.handle.net/10356/104532

https://doi.org/10.1089/ten.tea.2012.0507

TISSUE ENGINEERING: Part A
Volume 19, Numbers 9 and 10, 2013

DOI: 10.1089/ten.tea.2012.0507

A Mathematical Model Predicting the Coculture Dynamics of Endothelial and Mesenchymal Stem Cells for Tissue Regeneration

Yao Wang, BEng,[1,2,*] Tomer Bronshtein, PhD,[1,*] Udi Sarig, PhD,[1,2] Evelyne Bao-Vi Nguyen, BEng,[1,2] Freddy Yin Chiang Boey, PhD,[1] Subbu S. Venkatraman, PhD,[1] and Marcelle Machluf, PhD[1,2]

In most tissue engineering applications, understanding the factors affecting the growth dynamics of coculture systems is crucial for directing the population toward a desirable regenerative process. Yet, no comprehensive analysis method exists to quantify coculture population dynamics, let alone, a unifying model addressing the "environmental" factors influencing cell growth, all together. Here we suggest a modification of the *Lotka-Volterra* model to analyze the population dynamics of cocultured cells and predict their growth profiles for tissue engineering applications. This model, commonly used to describe the population dynamics of a prey and predator sharing a closed ecological niche, was found to fit our empirical data on cocultures of endothelial cells (ECs) and mesenchymal stem cells (MSCs) that have been widely investigated for their regenerative potential. Applying this model to cocultures of this sort allows us to quantify the effect that culturing conditions have on the way cell growth is affected by the same cells or by the other cells in the coculture. We found that in most cases, EC growth was inhibited by the same cells but promoted by MSCs. The principles resulting from this analysis can be used in various applications to guide the population toward a desired direction while shedding new light on the fundamental interactions between ECs and MSCs. Similar results were also demonstrated on complex substrates made from decellularized porcine cardiac extracellular matrix, where growth occurred only after coculturing ECs and MSCs together. Finally, this unique implementation of the *Lotka-Volterra* model may also be regarded as a roadmap for using such models with other potentially regenerative cocultures in various applications.

Introduction

Tissue engineering applications designed to achieve functional tissue replacements often require coculturing of several cell types harboring regenerative potential in the same or nearby physiological niches.[1,2] Understanding the growth dynamics of such cocultures, which is manifested in varying growth rates during the culturing period, is crucial for directing the population of interest toward a desirable regenerative process.[3–5] A number of "environmental" factors, independent of the cocultured cells but able to influence their growth rates, will eventually control their population dynamics. Factors such as cell seeding densities, seeding ratios, and medium composition, not only affect the growth rates of the cocultured cells themselves but may also change the way cells affect each other.[6]

Complex and important cocultures of this sort, made from simultaneously[7,8] or sequentially seeded[9,10] mesenchymal stem cells (MSCs) and endothelial cells (ECs), have been widely investigated for their pivotal regenerative potential to support a variety of cardiovascular applications in tissue engineering. MSCs cocultured with ECs were found to exhibit strong pro-angiogenic and vasculogenic effects that were associated with their ability to stabilize the formation of tubular vascular-like structures both *in vitro*[9,11] and *in vivo*.[12,13] MSCs were also shown, under certain *in-vitro* conditions, to trans-differentiate into ECs,[14–16] further reaffirming their *in-vivo* association. However, despite the ample literature reporting EC and stem cell cocultures,[3,5,17,18] no comprehensive investigation has explored and quantified their population dynamics, let alone investigated them together in a unifying model addressing the several factors influencing cell growth. Consequently, coculturing conditions such as medium composition, seeding densities, and ratios have been arbitrarily selected[9,18] or based on narrow

[1]NTU–Technion Biomedical Labs, School of Materials Science and Engineering, Division of Materials Technology, Nanyang Technological University, Singapore, Singapore.
[2]Faculty of Biotechnology and Food Engineering, Technion–Israel Institute of Technology, Haifa, Israel.
*The authors have contributed equally to this work.

optimizations[8] that were reported without detailed reasoning. Since blood supply of tissue constructs exceeding the diffusion barrier remains a critical problem,[19] shedding new light on the coculture dynamics of MSCs and ECs, two key players in angiogenesis and vasculogenesis,[20] should prove beneficial in cardiovascular applications.

Therefore, to guide ECs–MSCs or any other cocultured cells toward specific regenerative directions, favoring one cell over the other, an effort must be made to determine the effect of the culturing conditions on the population dynamics using a comprehensive mathematical model. Having a model at hand, able to predict coculture behavior under different initial conditions, may not only save valuable optimization time, but is also likely to provide insightful information on the mutual effects exerted by the cocultured cells. Such a model can be used to deduce quantitative measures that can be directly implemented in tissue engineering applications, sparing laborious educated guessing, which is mostly based on qualitative information that is widely reported, yet hardly comprehensive.

In this study, we established a two-dimensional (2D) coculture system of bone-marrow-derived MSCs and human umbilical vein endothelial cells (HUVECs), and determined the effect of medium composition, cell seeding density, and ratio on the growth and viability of the single-cultured and cocultured cells. We found that the *Lotka-Volterra* model, commonly used in population studies to describe the dynamics of two species (prey and predator) sharing a closed ecological niche,[21] can be modified to fit complex mammalian coculture systems. Accordingly, the *Lotka-Volterra* model was modified to account for the different metabolic rates of the cocultured cells and address the appropriate boundary conditions, which were set based on the initial seeding densities and ratios. This action allowed us to quantify the effect that culturing conditions might have on the way cell growth is inhibited or induced by the same cell type (self-effect) or by the other type (other-effect) in the coculture. This unique implementation of the *Lotka-Volterra* model on EC–MSC cocultures, which can be widely used in cardiovascular applications, may also be regarded as a roadmap for using such models with other potentially regenerative cells in various applications.

Materials and Methods

Cells and medium

Human bone marrow mesenchymal stem cells and HUVECs (Lonza™, Basel, Switzerland) were cultured using two types of media and their combinations: complete Lonza endothelial growth medium-2 (EGM-2)™, HUVEC-designated medium according to the literature[6,22]; and complete αMEM (minimum essential medium Eagle, alpha modification; Sigma-Aldrich™, St. Louis, MO), MSC-designated medium according to the literature,[23–26] supplemented with 10% Gibco® fetal bovine serum (FBS), 1% L-glutamine, 5 ng/mL basic fibroblast growth factor, and 1% antibiotic-antimycotic (Invitrogen™, Carlsbad, CA). All medium combinations are per volume of the complete medium. Media were replaced at least every 2 days. All tissue culture plates were treated with 0.1% gelatin (Sigma-Aldrich) in phosphate buffered saline (PBS) for at least 6 h at 37°C. Cells were cultured at 37°C in a humidified incubator with 5% CO_2.

Determining cell number and viability

Culture viability was determined using the AlamarBlue™ reagent (Invitrogen) according to the manufacturer's protocol,[27] and as published before,[28] using a Varioskan Flash spectral scanning multimode reader (Thermo-Fisher Scientific, Waltham, MA). AlamarBlue fluorescence intensities (FIs) were determined as measures of culture viability or converted to cell numbers (when applicable) using standard calibration curves under the same conditions.

The basal growth and metabolic rates of MSCs and HUVECs in various medium compositions

MSCs and HUVECs were seeded (5000 cells/well) in 24-well plates (NUNC®, Roskilde, Denmark) and cultured for 7 days in six combinations of complete MSC- and HUVEC-designated media: 100% αMEM, 80% αMEM + 20% EGM-2, 60% αMEM + 40% EGM-2, 40% αMEM + 60% EGM-2, 20% αMEM + 80% EGM-2, and 100% EGM-2. Cell numbers were determined using AlamarBlue. The cell growth rates, under each medium composition, were derived from their exponential growth phases with $R^2 > 0.95$. Cell metabolic rates were obtained as the AlamarBlue FI (per thousand cells) at the time of seeding—that is, the theoretical values elucidated from the intercept of the exponential growth curves with confidence levels larger than 99.99%.

Population dynamics of MSC and HUVEC cocultures

For coculture studies, MSCs and HUVECs were mixed into nine different ratios (5:1, 4:1, 3:1, 2:1, 1:1, 1:2, 1:3, 1:4, and 1:5) and seeded for a total density of 9000 cells/cm^2 in 96-well plates (NUNC). Cells were cultured for 7 days in three medium compositions: complete αMEM, complete EGM-2, and a 1:1 mix (v/v) of the above media. Coculture viability was measured daily using AlamarBlue. However, since the two cell types in our cocultures have different metabolic rates ($\varepsilon_{MSC} \neq \varepsilon_{HUVEC}$), their AlamarBlue readings (as raw FI values) cannot be correlated directly to population sizes (cell numbers) but only presented as measures of viability.[29] Further analysis was conducted by fitting the viability data onto the *Lotka-Volterra* model, which is commonly used in population studies to describe the dynamics of prey-and-predator species.[23,24] This unique implementation of the model, which is described in detail in the Supplementary Material: Part A (Supplementary Data are available online at www.liebertpub.com/tea), takes into account the different metabolic rates and can thus estimate the size of the different populations. Using this model, the population dynamics of two species (e.g., MSCs and HUVECs) sharing a closed ecological niche is governed by their basal growth rates (μ) and two additional parameters K and L for each species. Accordingly, the coefficients K_i and L_i describe the "self-effect" and the "other-effect" on the growth rate of cell type "i," respectively. For example, negative K values for MSCs ($K_{MSC} < 0$) indicates that MSC growth is inhibited by the MSCs themselves, while a positive L value for HUVECs ($L_{HUVEC} > 0$) indicates that HUVEC growth is encouraged by the MSCs in the coculture.

Phenotypic properties of cocultured MSCs and HUVECs

The expression of common MSC and HUVEC markers (CD105 and CD44) and HUVEC markers (CD31 and von

Willebrand factor [vWF]) was studied for MSCs, HUVECs, and 1:1 MSC and HUVEC cocultures. Cells were seeded in 10 cm tissue culture plates (9000 cells/cm^2), cultured for 7 days in complete EGM-2 (shown to best support both cell types), harvested, washed with PBS, permeabilized with 0.1% Triton X-100 (Sigma-Aldrich) in PBS and analyzed according to Santa Cruz Biotechnology flow cytometry protocol.[30] Briefly, permeabilized cells were incubated with primary antibodies: rabbit anti-human CD31 (1:50; Santa Cruz, CA), rabbit anti-human vWF (1:50; Santa Cruz), rat anti-human CD44 (1:50; BioLegend, San Diego, CA), and mouse anti-human CD105 (1:50; BD Biosciences, Franklin Lakes, NJ). Cells were then conjugated with fluorescently labeled (fluorescein isothiocyanate or phycoerythrin) secondary antibodies (1:50; Santa Cruz), acquired using the Guava easyCyte 6HT/2L System (Millipore, Billerica, MA), and analyzed using FlowJo™ flow cytometry analysis software (Tree Star Inc., Ashland, OR).

Population dynamics of MSC and HUVEC cocultures under low seeding densities

The final proportion of each subpopulation in the *Lotka-Volterra* model is affected not only by the culturing time and initial seeding ratios but also by the absolute population size at seeding time as well. To prove that our theoretical outcome agrees with the de facto behavior of the system, the population dynamics of MSC and HUVEC cocultures were studied using low seeding densities. MSCs, HUVECs, and 1:1 cocultures were seeded on 10 cm tissue culture plates at low initial densities (500 cells/cm^2) and cultured in complete EGM-2 for 7 days. Before seeding, MSCs were labeled with fluorescent membrane tracker DiI (Invitrogen) according to the manufacturer's protocol.[31] To evaluate population size, 7-day-old cocultures were followed up by flow cytometry (Millipore-Guava™), fluorescent microscopy, and light contrast microscopy (DIC) using ECLIPSE Ti microscope (Nikon Instruments Inc., Melville, NY).

Effects of seeding density and medium volume on the population dynamics of MSC and HUVEC cocultures

HUVECs and MSCs mixed in a 1:1 ratio were seeded on tissue culture plates with different culture areas (NUNC; 12, 24, and 48 wells) to achieve three seeding densities: 1000, 1500, and 3000 cells/cm^2. The total number of cells per well was maintained constant. Cells were then cultured for up to 7 days in either 1 or 0.2 mL of complete EGM-2 that was replenished daily; their viability was evaluated using AlamarBlue.

Population dynamics of HUVEC and MSC cocultures on 3D scaffolds

Cylindrical slices of decellularized porcine cardiac left-ventricle extracellular matrix (ECM) (0.3 cm thick with a surface area of 0.5 cm^2) were obtained, placed in 96-well low binding plates (NUNC), and re-seeded as previously reported by us.[26] For simultaneous cocultures, a total number of 300,000 HUVECs, MSCs, or a 1:1 mixture of the two were prepared in 40 μL complete EGM-2 and seeded on top of each ECM slice. The cells were allowed to attach for 90 min in culturing conditions, followed by a brief wash with PBS. Seeded ECM slices were then transferred to 24-well low binding plates (1 slice/well) and cultured in complete EGM-2 for 14 days. In sequential coculture, 150,000 MSCs were first seeded on the ECM slices (as described above) and cultured for 7 days, following which 150,000 HUVECs were seeded "on top" of the MSCs and cultured for an additional 7 days. Cell viability was determined using AlamarBlue and translated into cell numbers according to standard calibration curves for each cell type grown on the same substrate.

Statistical analysis

Results are expressed as mean ± SD ($n \geq 3$). Statistical significance in the differences of the means was evaluated by a two-sided *t*-test. Analysis of variance was used to test the statistical significance of differences among groups. For results derived from fitted correlations, a correlation coefficient of $R^2 > 0.95$ was required to include the results into our analysis. Coefficients resulting from nonlinear correlation are presented without standard deviation and only if they reflect an effect with $p < 0.01$. Model errors are presented as confidence intervals on the Supplementary Data.

Results

The basal growth rates and metabolic rates of MSCs and HUVECs under various media

Medium composition had no effect on the growth rates of MSCs (Fig. 1a), which exhibited an average basal growth rate of 0.77 ± 0.05 [$^1/_{\text{day}}$] that remained higher than HUVEC growth rates under all medium compositions. HUVECs, on the other hand, were significantly affected by medium composition ($p < 0.001$) and exhibited no growth under 100% αMEM, but a significant increase in growth rates under 20%–100% EGM-2. The metabolic rates of both cell types increased ($p < 0.001$) as the EGM-2 proportion increased, with HUVECs exhibiting higher values than MSCs in all medium compositions (Fig. 1b).

The population dynamics of MSC and HUVEC cocultures under various media

MSCs did not exhibit a significant self-effect (Fig. 2a) under any medium composition ($K_{\text{MSC}} = 0$, $p > 0.05$), while HUVECs always exhibited a self-inhibitory effect ($K_{\text{HUVEC}} < 0$, $p < 0.01$). This self-inhibitory effect was much weaker in the complete HUVEC-designated medium ($K_{\text{HUVEC,EGM-2}} = -0.02$ [1000 cells $*$ day]$^{-1}$) than in any other medium composition ($K_{\text{HUVEC}} = -0.16 \pm 0.01$ [1000 cells $*$ day]$^{-1}$). MSC growth was inhibited by HUVECs only in the complete MSC-designated medium (Fig. 2b) with $L_{\text{MSC},\alpha\text{MEM}} = -0.15$ [1000 cells $*$ day]$^{-1}$ ($p < 0.05$). The growth of HUVECs, on the other hand, was significantly encouraged ($p < 0.05$) by MSCs in both the HUVEC-designated medium and the 1:1 mix of the two media ($L_{\text{HUVEC},\alpha\text{MEM}} < L_{\text{HUVEC,MIX}} < L_{\text{HUVEC,EGM-2}} = 0.075$ [1000 cells $*$ day]$^{-1}$). After elucidating the model coefficients (i.e., *K* and *L*) for each cell type under each medium composition, we simulated the size of each population. The simulation is demonstrated for initial seeding density of 3000 cells per well (in a 96-well plate) using a 1:1 MSC to HUVEC ratio grown for 7 days in the complete MSC-designated medium (Fig. 2c), a 1:1 mix (Fig. 2d) and the complete HUVEC-designated medium (Fig. 2e).

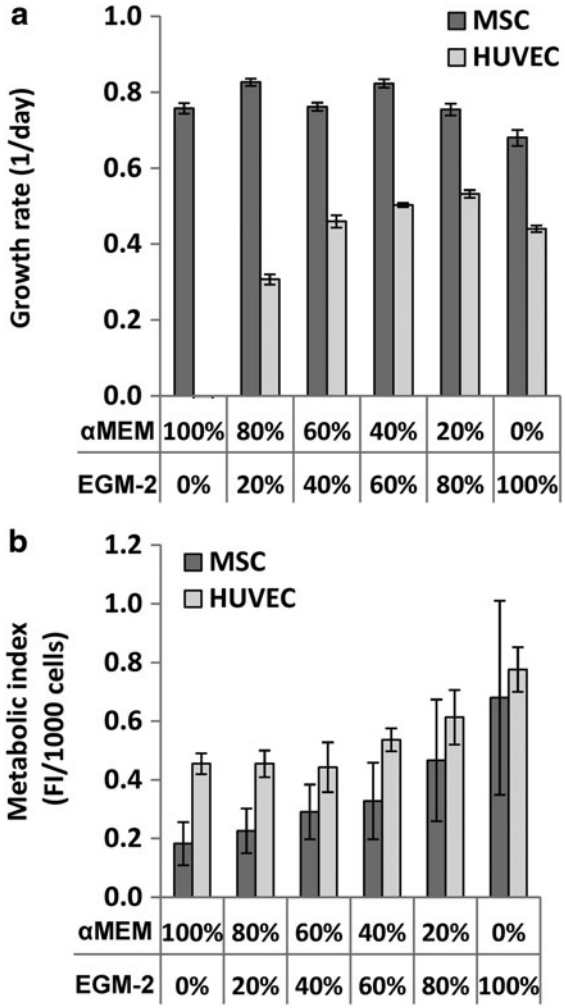

FIG. 1. Growth rates and metabolic indices of mesenchymal stem cells (MSCs) and human umbilical vein endothelial cells (HUVECs) under various medium compositions. Growth rates of MSCs and HUVECs ($n=5$) under various medium compositions ranging from 100% complete αMEM to 100% complete endothelial growth medium-2 (EGM-2) **(a)**. The cells' metabolic indices ($n=5$) as AlamarBlue fluorescence intensities at time ZERO per 1000 cells plotted versus medium composition **(b)**. αMEM, minimum essential medium Eagle, alpha modification.

Phenotypic properties of MSCs and HUVECs cocultured in the HUVEC-designated medium

MSCs expressed common MSC and HUVEC markers (CD105 and CD44), but not the unique HUVEC markers (CD31 and vWF; Fig. 3a). HUVECs, as expected, expressed all four markers (Fig. 3b). The expression profiles of 7-day 1:1 MSC and HUVEC cocultures were identical to those of HUVECs alone (Fig. 3c).

Population dynamics of MSC and HUVEC cocultures under low seeding densities

MSCs (fluorescently labeled with DiI), HUVECs, and a 1:1 MSC and HUVEC coculture were seeded at much lower densities than before (300 cells/cm^2), grown for 7 days in the

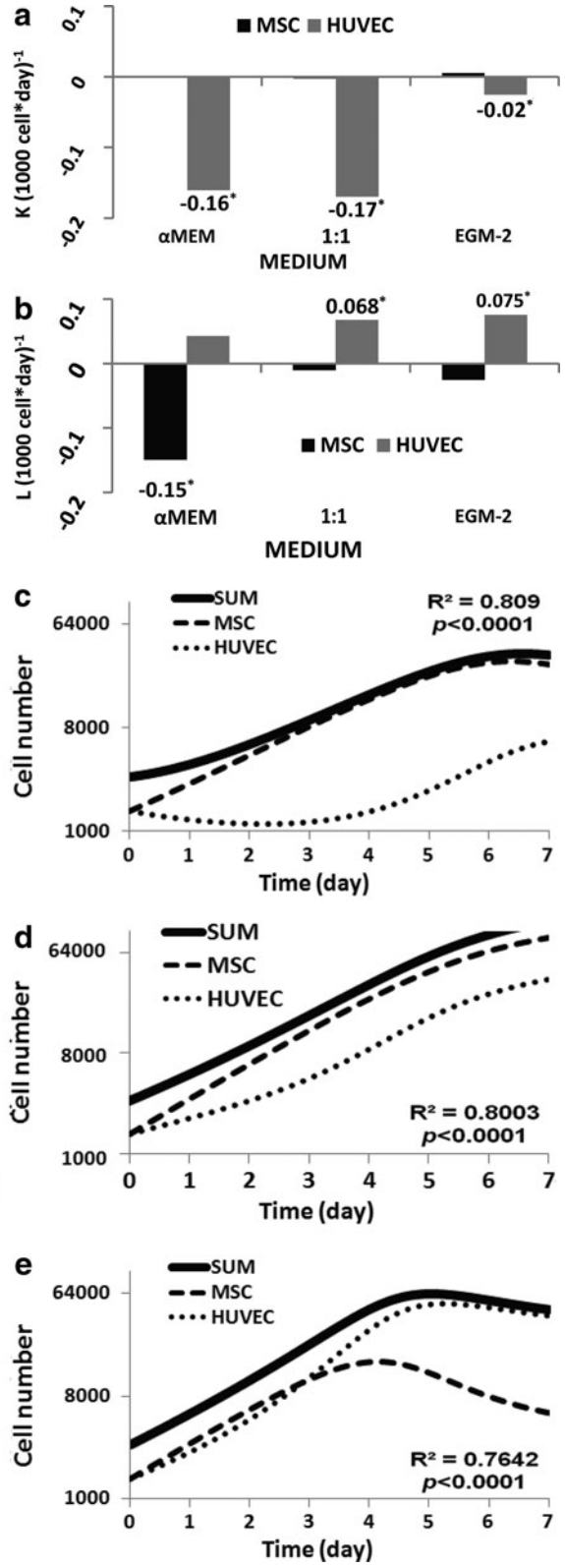

FIG. 2. Population dynamics of MSCs and HUVECs cocultured under different medium compositions. Self- **(a)** and other-effect **(b)** of cocultured MSCs and HUVECs according to the *Lotka-Volterra* model under various medium compositions. Significant effects are indicated by data labels and asterisks. Predicted cell numbers using the model under αMEM **(c)**, 1:1 (v/v) mix **(d)**, and EGM-2 **(e)**.

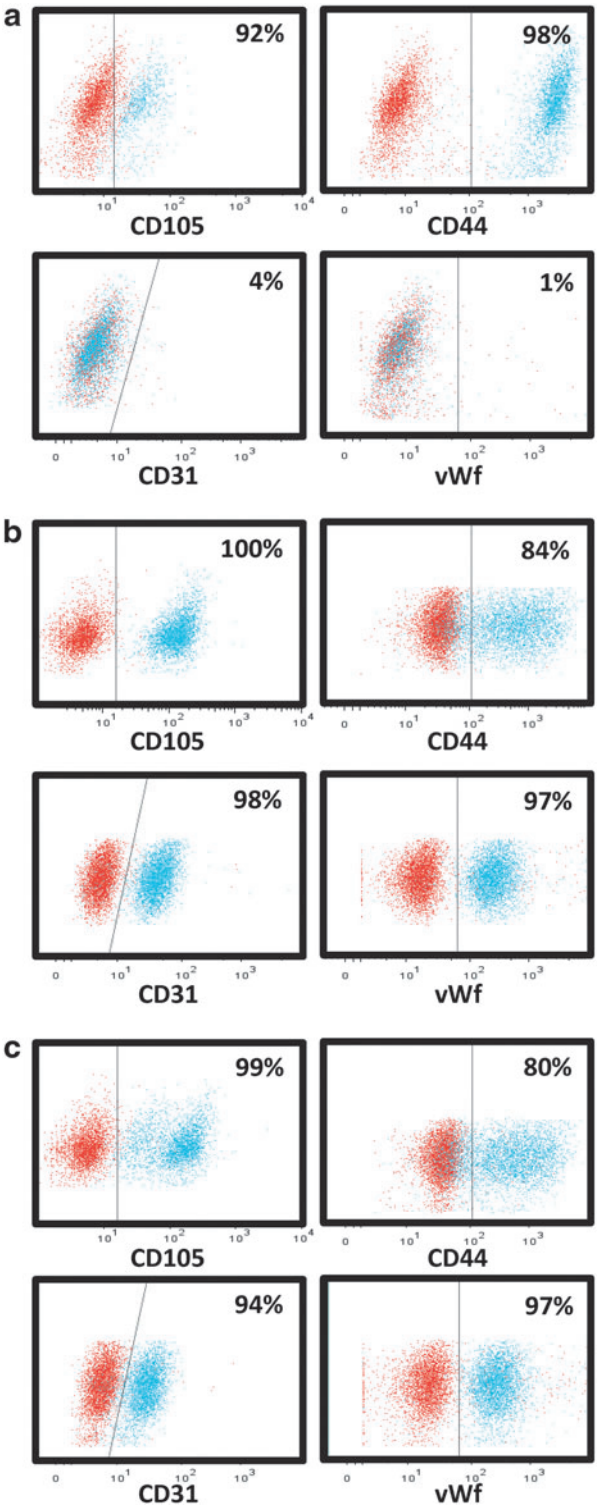

FIG. 3. Fluorescence activated cell sorting (FACS) analysis of MSC and HUVEC cocultures. Expression of CD105, CD44, CD31, and von Willebrand factor (vWF) by MSCs **(a)**, HUVECs **(b)**, and 1:1 coculture **(c)** grown for 7 days. Representative results ($n = 3$) depicted as forwards scatter versus fluorescence intensity. Percentages refer to positive populations (blue) under identical gates (per marker) determined according to the isotype control (red).

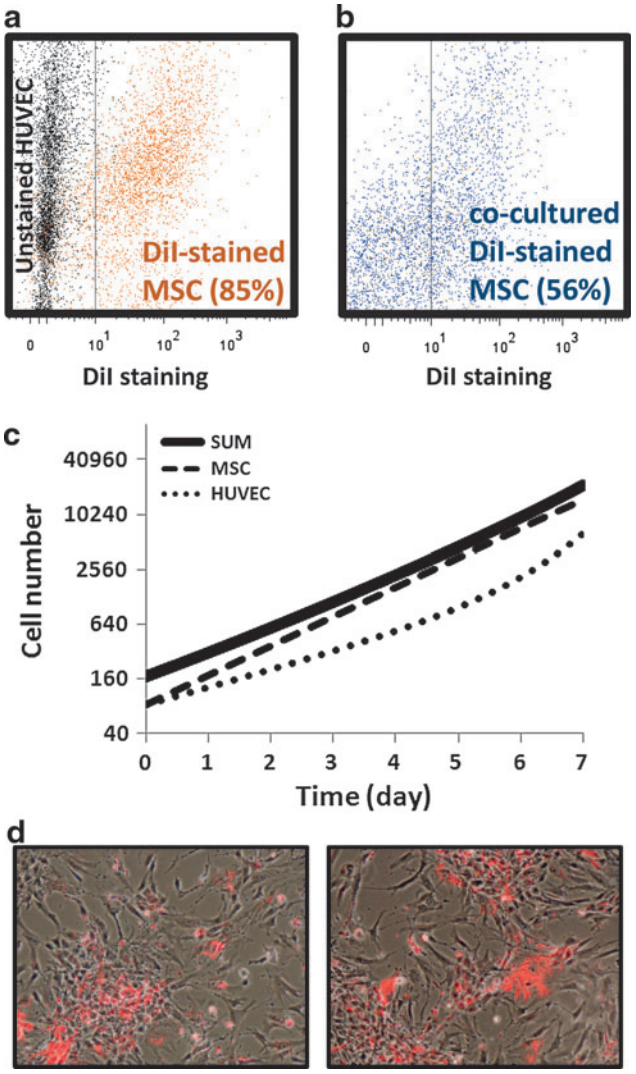

FIG. 4. MSCs and HUVECs cocultured under low seeding densities. FACS analysis of separately grown unstained HUVECs and DiI-labeled MSCs (overlay) **(a)** and a 1:1 coculture **(b)**. Simulated coculture growth under the same conditions **(c)**. Coculture fluorescently imaged **(d)**. Cells were seeded at low densities and grown for 7 days. Representative results ($n = 3$) are depicted.

complete HUVEC medium, and analyzed by fluorescence activated cell sorting (FACS). DiI labeling integrity was validated as described in detail in the Supplementary Material: Part B. Figure 4a shows two distinct populations (in terms of DiI labeling) when overlaying the results for unlabeled HUVECs and DiI-labeled MSCs that were cultured separately for 7 days. However, analysis of the 7-day coculture (Fig. 4b) revealed only one population with 56% DiI-positive cells. Dividing the ratio of DiI-positive cells in the coculture (Fig. 4b, 56%) by the ratio of DiI-positive cells in the control samples (DiI-stained MSCs, Fig. 4a, 85%) produces a normalized ratio of 66% MSCs in the coculture after 7 days. This fraction of MSCs in the coculture (66%) agrees strikingly with the MSC proportion anticipated by the model with low seeding densities (71%). Based on the model, the derived MSC and HUVEC populations on day 7 have 15,000

and 6000 cells, respectively (Fig. 4c). Supporting images of the same low-density cocultures, after 7 days, also reveal a much larger proportion of DiI-labeled MSCs (Fig. 4d) than the one previously observed in high-density seeded cocultures.

Effects of seeding density and medium volume on the population dynamics of MSC and HUVEC cocultures

Coculture growth rates were found to be inversely proportional to the seeding densities in both high (Fig. 5a) and low medium volumes (Fig. 5b), excluding the high-density seeded cells, showing almost no growth under low medium volume.

The growth of HUVEC and MSC cocultures on 3D scaffolds

No variations were found in the population sizes between separately and simultaneously cocultured cells ($p > 0.05$) grown on complex 3D porcine cardiac extracellular matrix scaffolds that decreased until day 4, from which point they remained constant (Fig. 6a). However, in the sequential coculture, where HUVECs were seeded on top of MSCs, significant growth ($p < 0.01$) of more than twofold was observed on the following 7 days (Fig. 6b).

Discussion

Cocultures of two or more cell types are frequently used in tissue engineering to initiate or support certain regenerative processes.[20] Out of many different combinations of cells possessing regenerative potential, EC and MSC cocultures are among the most investigated for cardiovascular applications.[9,18] As recently discovered, when cocultured with ECs, MSCs exhibit the ability to actively interact with and support the formation of vascular tubular arrays.[9,14,20,32,33] Despite their popularity, however, the population dynamics of EC–MSC cocultures are still unclear.[17] The factors governing these dynamics have not been thoroughly quantified even in respect to the most fundamental effectors such as medium composition, seeding density, and cell seeding ratios, let alone in a comprehensive model that combines two or more of the above effectors.

When cocultured together, most literary publications report the use of either complete HVUEC[9,34] or MSC media[20] to support both cell types grown in the same niche. These media, commonly used without detailed reasoning and explanation, are not necessarily optimal for all coculture applications. Therefore, and in order to guide the cocultured populations toward a desirable regenerative direction, an effort must be made to understand and quantify the effect of many factors on single and cocultured cells. Most importantly, factors such as the seeding density and ratios, making up the model boundary conditions, as well as the medium composition, not only affect the cells themselves but also change the way the cells affect each other. Moreover, in order to estimate the size of each subpopulation, any applied model should resolve the term "viability," which is commonly used instead of cell number,[35] as the AlamarBlue measurements of the cocultured cells cannot be resolved to reflect on the cell number of each component separately.[36]

In light of the substantial therapeutic potential associated with cocultures of this sort, and due to the difficulties in analyzing such complex systems, often with limited success,[17,37] a comprehensive mathematical model, which can provide quantitative analysis and reliable prediction of coculture behavior, is required to facilitate future applications. Interestingly, taking cell seeding density and ratios into account, we found that the *Lotka-Volterra* model was highly correlated with our empirical coculture viability data. The *Lotka-Volterra* model is regularly used in population studies to describe the dynamics of two species, often regarded as prey and predator sharing the same ecological niche and exerting mutual effects.[21] Beyond using the initial seeding densities and ratios as boundary conditions, the model was modified to include the cells' metabolic rates, elucidated from single cultures, which were used to "translate" the raw viability data into cell numbers reflecting the populations' sizes. According to this model, two effects are defined for each species (e.g., MSCs or HUVECs), the "self-effect" that one species exerts upon itself and the "other-effect"

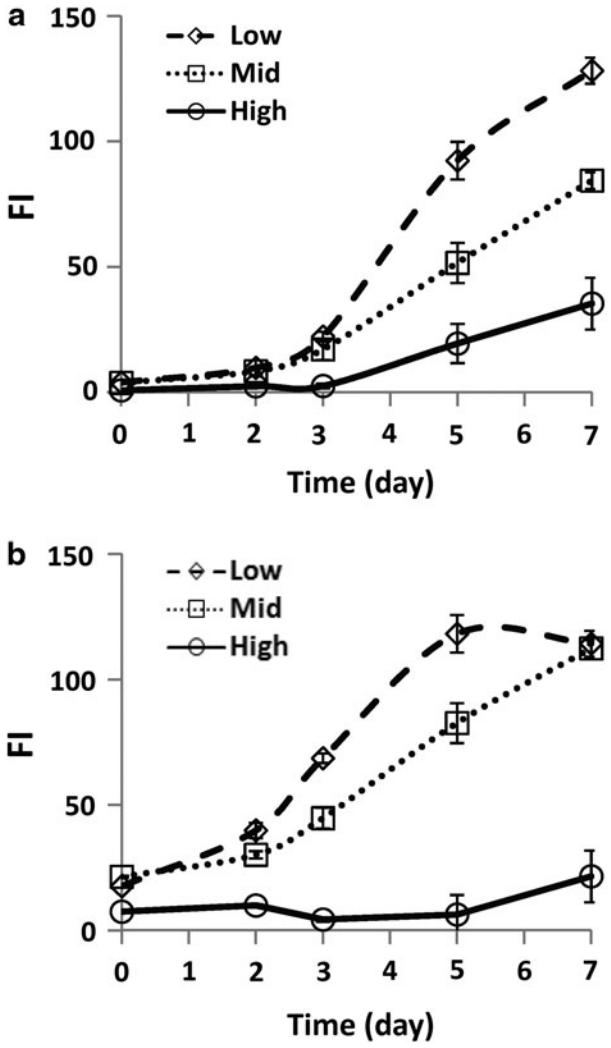

FIG. 5. Seeding density effect on coculture growth. The overall average viability of cells seeded 1:1 (HUVEC-to-MSC) on plates with different culturing areas to achieve three seeding densities: LOW: 1000, MED: 1500, and HIGH: 3000 cells/cm^2 and grown for 7 days in 1 **(a)** or 0.2 mL **(b)** media that were replenished every day. FI, fluorescence intensity.

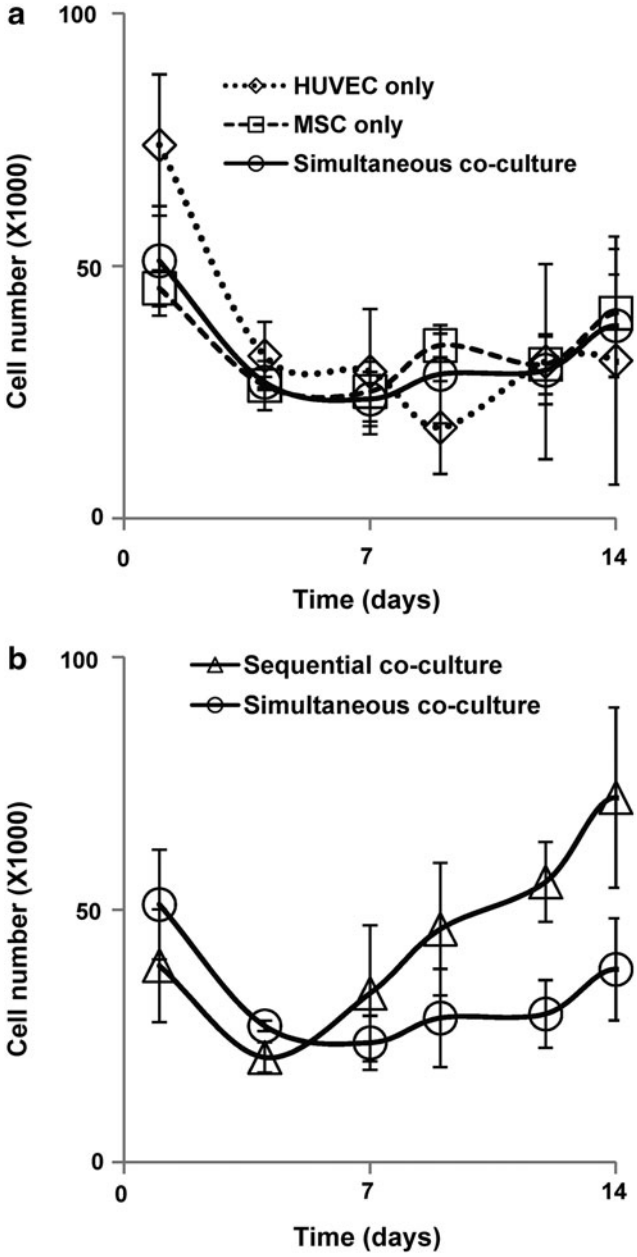

FIG. 6. MSCs and HUVECs cocultured on three-dimensional substrates. Simultaneous cocultures (MSCs and HUVECs together from day 0) grown on decellularized porcine cardiac extracellular matrix (ECM) compared to separately cultured cells **(a)**. Simultaneous cocultures compared with sequential ones made by reseeding the ECMs with HUVECs on top of the MSCs that were grown separately for 7 days **(b)**.

according to which one species is affected by the other. This model, which has never been applied to human cells, was used previously to describe interactions within different microbial and mammalian cells,[38,39] and can probably be extended to other coculture systems harboring regenerative potential.

Fitting the *Lotka-Volterra* model to our data reveals that HUVECs exerted an inhibitory self-effect under all medium compositions, especially in non-HUVEC-designated media while MSCs exhibited no self-effect. These results agree with the "stemmy," immortal, and high-proliferative nature of MSCs, which are supposed to populate their target niche with minimal self-effect while being more influenced by their surroundings, leading them to their final differentiated state.[40] HUVECs, on the other hand, are expected to be self-inhibited in low vascular endothelial growth factor concentrations,[41] so as not to overgrow and hamper the monolayer morphology of the vascular intima.[42] As for the other-effect, MSC growth was unaffected by HUVECs in both the HUVEC-designated medium and the 1:1 mix, which observation can be also attributed to their "stemmy" nature. However and rather surprisingly, MSCs were inhibited by HUVECs in MSC-designated medium; nevertheless, they were eventually shown to dominate the coculture owing to their much higher basal growth rate. The growth rate of HUVECs, on the other hand, was increased by MSCs in both the HUVEC-designated medium and the 1:1 mix, which phenomenon can be attributed to MSCs regulatory effect over ECs.[9,34]

In accordance with the model predictions, FACS analysis of densely seeded cells, cocultured (1:1) for 7 days under a complete HUVEC medium, revealed a population that was entirely dominated by cells expressing all HUVEC markers with no apparent traces of MSCs. Unlike the separately cultured cells, which maintained their original markers, MSCs seemed to disappear when cocultured with HUVECs under these conditions. Microscopy imaging of fluorescently labeled MSCs, separately cultured and cocultured with HUVECs (Supplementary Material: Part C), further supports MSC depletion rather than MSC trans-differentiation, which is unlikely to occur within a short period of 7 days.[15,20] Though the exact mechanism causing this effect is poorly understood,[37] these counterintuitive results were predicted by the model presented herein, and further substantiate its validity.

Being able to measure how the medium composition changes the self- and other-effects, and given the initial seeding density and ratios, being able to predict the size of each subpopulation along the coculturing period does away with the need for costly optimizations. Yet, it remains clear that for most biomedical purposes, ECs–MSCs will still be applied on complex 3D substrates[9,20,32,33] that by geometry alone may change the population dynamics from what is seen on standard 2D tissue culture plates.[34] However, as important as they may be, the substrate material and geometry are not the sole factors governing the population dynamics.[17] Other equally important factors, such as the ones addressed here, also affect the population dynamics on a variety of substrates.[33,34] Therefore, we believe that optimizing these factors under standard conditions can serve as valuable reference points for more complex substrates.

To further validate our model, a second batch of cocultures were attempted with 95% lower seeding densities, analyzed, and compared to the model predictions. FACS analysis and microscopy imaging of separately and cocultured cells revealed a striking agreement between the final proportion of MSCs, determined by flow cytometry (66%), and the one predicted by the model (71%). The same MSCs that were shown before to vanish from densely seeded cocultures were found to dominate cocultures seeded in low densities. These entirely different dynamics, exhibited by cells cocultured under different seeding densities, can be

attributed to the distance effect on the migration and cross-talk between cells, which are largely affected by the short half-life of the chemokines that mediate such interactions.[32]

While maintaining the same medium volume and total cell number, an inverse correlation was found between the seeding density and the growth rate. Apart from the high density-seeded cells, which probably suffered stress under a low medium volume, a similar inverse proportion was also found between the growth rate and the medium volume—implying an inhibitory effect due to dilution of growth enhancing soluble factors. Our results so far, demonstrating that a more concentrated paracrine effect with less physical interaction leads to higher growth rates, may also correspond with physiological conditions in which the two cell types are physically separated by semipermeable buffers such as the blood vessel ECM and others.[32]

Preliminary cocultures were also attempted on a complex 3D substrate made of porcine left-ventricle cardiac acellular ECM that was previously suggested as a promising scaffold for tissue engineering[43] and that is widely investigated in our group for cardiac regeneration therapies.[26,44] Our results so far demonstrate that on such highly geometrically and chemically complex material, the order of seeding is also of highly significant. Whereas some cell survival was observed with separately cultured or simultaneously cocultured cells, only a sequential coculture of MSCs topped up with HUVECs exhibited significant growth. These results may suggest that on such scaffolds, MSCs not only support HUVEC growth but are also required to prepare the physiological niche before HUVEC establishment, probably by rearranging the ECM and providing the HUVECs with better "docking sites."[5]

Other interesting and important mathematical models were reported in the literature to describe the dynamic growth of MSCs or embryonic stem cells. Tabatabai *et al.* applied a hyperbolastic growth model to explain the low proliferation of MSCs under osteonecrotic conditions.[45] Though cell renewal, differentiation, and proliferation were taken into consideration in this model, external factors such as nutrients, space, and interaction with other cell types, were not included. Some of these external factors affecting MSC growth were accounted for in earlier studies using population-balancing modeling, although in 2D conditions and monocultures only.[46] To the best of our knowledge, here we present the first study that models the population dynamics of MSC–EC cocultures in a comprehensive manner taking both cellular and environmental factors into account, on both simple and complex substrates. After resolving the macro properties affecting coculture growth, our results definitely merit further research into the effect of the biochemical properties of the substrate that were shown to alter coculture dynamics as well.[47]

In conclusion, based on our studies in standard conditions, HUVECs and MSCs under coculture conditions were shown to exhibit competitive prey-and-predator behavior with substantial mutual effects that were largely affected by the medium composition. By applying the *Lotka-Volterra* model for such systems, the effects of culturing parameters on the population dynamics can be understood and predicted in, but not limited to, a 2D environment. The elucidated and now quantified relations between the culturing condition and the cells' mutual interactions may not only serve as an insightful guideline for 3D studies but is likely to enhance the research into the underlying mechanism governing population dynamics, which may be applied in numerous applications in regenerative medicine.

Acknowledgments

This research is supported by the Singapore National Research Foundation under the CREATE program; The Regenerative Medicine Initiative in Cardiac Restoration Therapy Research Program; and The Israel Science Foundation under grant No. 1563/10 entitled "Thick acellular heart ECM with inherent vasculature: Towards engineering cardiac tissue replacement." The authors wish to thank Dr. Susan Liao and Dr. Priyadarshini S. Mhaisalkar for their help and assistance.

Disclosure Statement

No competing financial interests exist.

References

1. Muschler, G.F., Nakamoto, C., and Griffith, L.G. Engineering principles of clinical cell-based tissue engineering. J Bone Joint Surg Am **86-A,** 1541, 2004.
2. Dahan, N., Zarbiv, G., Sarig, U., Karram, T., Hoffman, A., and Machluf, M. Porcine small diameter arterial extracellular matrix supports endothelium formation and media remodeling forming a promising vascular engineered biograft. Tissue Eng Part A **18,** 411, 2012.
3. Ball, S.G., Shuttleworth, A.C., and Kielty, C.M. Direct cell contact influences bone marrow mesenchymal stem cell fate. Int J Biochem Cell Biol **36,** 714, 2004.
4. Le Visage, C., Dunham, B., Flint, P., and Leong, K.W. Coculture of mesenchymal stem cells and respiratory epithelial cells to engineer a human composite respiratory mucosa. Tissue Eng **10,** 1426, 2004.
5. Hirschi, K.K., Rohovsky, S.A., and D'Amore, P.A. PDGF, TGF-beta, and heterotypic cell-cell interactions mediate endothelial cell-induced recruitment of 10T1/2 cells and their differentiation to a smooth muscle fate. J Cell Biol **141,** 805, 1998.
6. Loomer, P.M., Ellen, R.P., and Tenenbaum, H.C. Osteogenic and osteoclastic cell interaction: development of a co-culture system. Cell Tissue Res **294,** 99, 1998.
7. Meury, T., Verrier, S., and Alini, M. Human endothelial cells inhibit BMSC differentiation into mature osteoblasts *in vitro* by interfering with osterix expression. J Cell Biochem **98,** 992, 2006.
8. Villars, F., Guillotin, B., Amedee, T., Dutoya, S., Bordenave, L., Bareille, R., and Amedee, J. Effect of HUVEC on human osteoprogenitor cell differentiation needs heterotypic gap junction communication. Am J Physiol Cell Physiol **282,** C775, 2002.
9. Sorrell, J.M., Baber, M.A., and Caplan, A.I. Influence of adult mesenchymal stem cells on *in vitro* vascular formation. Tissue Eng Part A **15,** 1751, 2009.
10. Williams, C., and Wick, T.M. Perfusion bioreactor for small diameter tissue-engineered arteries. Tissue Eng **10,** 930, 2004.
11. Gruber, R., Kandler, B., Holzmann, P., Vogele-Kadletz, M., Losert, U., Fischer, M.B., and Watzek, G. Bone marrow stromal cells can provide a local environment that favors migration and formation of tubular structures of endothelial cells. Tissue Eng **11,** 896, 2005.

12. Asahara, T., Masuda, H., Takahashi, T., Kalka, C., Pastore, C., Silver, M., Kearne, M., Magner, M., and Isner, J.M. Bone marrow origin of endothelial progenitor cells responsible for postnatal vasculogenesis in physiological and pathological neovascularization. Circ Res **85,** 221, 1999.
13. Al-Khaldi, A., Eliopoulos, N., Martineau, D., Lejeune, L., Lachapelle, K., and Galipeau, J. Postnatal bone marrow stromal cells elicit a potent VEGF-dependent neoangiogenic response *in vivo*. Gene Ther **10,** 621, 2003.
14. Davani, S., Marandin, A., Mersin, N., Royer, B., Kantelip, B., Herve, P., Etievent, J.P., and Kantelip, J.P. Mesenchymal progenitor cells differentiate into an endothelial phenotype, enhance vascular density, and improve heart function in a rat cellular cardiomyoplasty model. Circulation **108 Suppl 1,** II253, 2003.
15. Oswald, J., Boxberger, S., Jorgensen, B., Feldmann, S., Ehninger, G., Bornhauser, M., and Werner, C. Mesenchymal stem cells can be differentiated into endothelial cells *in vitro*. Stem Cells **22,** 377, 2004.
16. Xu, Y., Meng, H., Li, C., Hao, M., Wang, Y., Yu, Z., Li, Q., Han, J., Zhai, Q., and Qiu, L. Umbilical cord-derived mesenchymal stem cells isolated by a novel explantation technique can differentiate into functional endothelial cells and promote revascularization. Stem Cells Dev **19,** 1511, 2010.
17. Kolbe, M., Xiang, Z., Dohle, E., Tonak, M., Kirkpatrick, C.J., and Fuchs, S. Paracrine effects influenced by cell culture medium and consequences on microvessel-like structures in cocultures of mesenchymal stem cells and outgrowth endothelial cells. Tissue Eng Part A **17,** 2199, 2011.
18. Lozito, T.P., Kuo, C.K., Taboas, J.M., and Tuan, R.S. Human mesenchymal stem cells express vascular cell phenotypes upon interaction with endothelial cell matrix. J Cell Biochem **107,** 714, 2009.
19. Kaully, T., Kaufman-Francis, K., Lesman, A., and Levenberg, S. Vascularization—the conduit to viable engineered tissues. Tissue Eng Part B Rev **15,** 159, 2009.
20. Au, P., Tam, J., Fukumura, D., and Jain, R.K. Bone marrow-derived mesenchymal stem cells facilitate engineering of long-lasting functional vasculature. Blood **111,** 4551, 2008.
21. Bailey, J.E., and Ollis, D.F. Biochemical Engineering Fundamentals. New York: McGraw-Hill, 1986.
22. Levenberg, S., Rouwkema, J., Macdonald, M., Garfein, E.S., Kohane, D.S., Darland, D.C., Marini, R., van Blitterswijk, C.A., Mulligan, R.C., D'Amore, P.A., and Langer, R. Engineering vascularized skeletal muscle tissue. Nat Biotechnol **23,** 879, 2005.
23. Lotka, A.J. Elements of Physical Biology. Baltimore: Williams & Wilkins, 1925.
24. Volterra, V. Variazioni e fluttuazioni del numero d'individui in specie animali conviventi. Rome: Mem. Accad. Lincei., 1927.
25. Sekiya, I., Larson, B.L., Smith, J.R., Pochampally, R., Cui, J.G., and Prockop, D.J. Expansion of human adult stem cells from bone marrow stroma: conditions that maximize the yields of early progenitors and evaluate their quality. Stem Cells **20,** 530, 2002.
26. Sarig, U., Au-Yeung, G.C., Wang, Y., Bronshtein, T., Dahan, N., Boey, Y.C., Subbu, V.S., and Machluf, M. Thick acellular heart extracellular matrix with inherent vasculature: potential platform for myocardial tissue regeneration. Tissue Eng Part A **18,** 2125, 2012.
27. AlamarBlue® Cell Viability Assay Protocol. Life Technologies. 2011. www.invitrogen.com/site/us/en/home/References/protocols/cell-and-tissue-analysis/cell-profilteration-assay-protocols/cell-viability-with-alamarblue.html#4.
28. Bronshtein, T., Toledano, N., Danino, D., Pollack, S., and Machluf, M. Cell derived liposomes expressing CCR5 as a new targeted drug-delivery system for HIV infected cells. J Control Release **151,** 139, 2011.
29. Gloeckner, H., Jonuleit, T., and Lemke, H.D. Monitoring of cell viability and cell growth in a hollow-fiber bioreactor by use of the dye Alamar Blue. J Immunol Methods **252,** 131, 2001.
30. Flow Cytometry Protocol. Santa Cruz Biotechnology, Inc. 2011. www.scbt.com/protocol_flow_cytometry.html.
31. Vybrant® DiI cell-labeling solution. Life Technologies. 2011. http://products.invitrogen.com/ivgn/product/V22885?ICID=search-product.
32. Trkov, S., Eng, G., Di Liddo, R., Parnigotto, P.P., and Vunjak-Novakovic, G. Micropatterned three-dimensional hydrogel system to study human endothelial-mesenchymal stem cell interactions. J Tissue Eng Regen Med **4,** 205, 2010.
33. Verseijden, F., Posthumus-van Sluijs, S.J., Pavljasevic, P., Hofer, S.O., van Osch, G.J., and Farrell, E. Adult human bone marrow- and adipose tissue-derived stromal cells support the formation of prevascular-like structures from endothelial cells *in vitro*. Tissue Eng Part A **16,** 101, 2010.
34. Traktuev, D.O., Merfeld-Clauss, S., Li, J., Kolonin, M., Arap, W., Pasqualini, R., Johnstone, B.H., and March, K.L. A population of multipotent CD34-positive adipose stromal cells share pericyte and mesenchymal surface markers, reside in a periendothelial location, and stabilize endothelial networks. Circ Res **102,** 77, 2008.
35. Cook, J.A., and Mitchell, J.B. Viability measurements in mammalian cell systems. Anal Biochem **179,** 1, 1989.
36. Nakayama, G.R., Caton, M.C., Nova, M.P., and Parandoosh, Z. Assessment of the Alamar Blue assay for cellular growth and viability *in vitro*. J Immunol Methods **204,** 205, 1997.
37. Duffy, G.P., Ahsan, T., O'Brien, T., Barry, F., and Nerem, R.M. Bone marrow-derived mesenchymal stem cells promote angiogenic processes in a time- and dose-dependent manner *in vitro*. Tissue Eng Part A **15,** 2459, 2009.
38. McLean, A.R., Rosado, M.M., Agenes, F., Vasconcellos, R., and Freitas, A.A. Resource competition as a mechanism for B cell homeostasis. Proc Natl Acad Sci U S A **94,** 5792, 1997.
39. Vereecken, K.M., Dens, E.J., and Van Impe, J.F. Predictive modeling of mixed microbial populations in food products: evaluation of two-species models. J Theor Biol **205,** 53, 2000.
40. Malgieri, A., Kantzari, E., Patrizi, M.P., and Gambardella, S. Bone marrow and umbilical cord blood human mesenchymal stem cells: state of the art. Int J Clin Exp Med **3,** 248, 2010.
41. Cao, R., Brakenhielm, E., Pawliuk, R., Wariaro, D., Post, M.J., Wahlberg, E., Leboulch, P., and Cao, Y. Angiogenic synergism, vascular stability and improvement of hind-limb ischemia by a combination of PDGF-BB and FGF-2. Nat Med **9,** 604, 2003.
42. Kazakoff, P.W., McGuire, T.R., Hoie, E.B., Cano, M., and Iversen, P.L. An *in vitro* model for endothelial permeability: assessment of monolayer integrity. In Vitro Cell Dev Biol Anim **31,** 846, 1995.
43. Badylak, S.F., Freytes, D.O., and Gilbert, T.W. Extracellular matrix as a biological scaffold material: structure and function. Acta Biomater **5,** 1, 2009.
44. Eitan, Y., Sarig, U., Dahan, N., and Machluf, M. Acellular cardiac extracellular matrix as a scaffold for tissue engineering:

in vitro cell support, remodeling, and biocompatibility. Tissue Eng Part C Methods **16,** 671, 2010.
45. Tabatabai, M.A., Bursac, Z., Eby, W.M., and Singh, K.P. Mathematical modeling of stem cell proliferation. Med Biol Eng Comput **49,** 253, 2011.
46. Mancuso, L., Liuzzo, M.I., Fadda, S., Pisu, M., Cincotti, A., Arras, M., Desogus, E., Piras, F., Piga, G., La Nasa, G., Concas, A., and Cao, G. Experimental analysis and modelling of *in vitro* proliferation of mesenchymal stem cells. Cell Prolif **42,** 602, 2009.
47. Wang, Y., Bronshtein, T., Sarig, U., Boey, F.Y.C., Venkatraman, S.S., and Machluf, M. Endothelialization of acellular porcine ECM with chemical modification. Int J Biosci Biochem Bioinform **2,** 363, 2012.

Address correspondence to:
Marcelle Machluf, PhD
Faculty of Biotechnology and Food Engineering
Technion IIT
Kiryat Hatechnion
Haifa 32000
Israel

E-mail: machlufm@tx.technion.ac.il

Received: August 21, 2012
Accepted: November 16, 2012
Online Publication Date: January 16, 2013